Electronic Supplementary Material (ESI) for Dalton Transactions.

Supplementary Information

An alkynyl-protected $Ag_{13-x}Cu_{6+x}$ nanocluster for catalytic hydrogenation

Yan-Li Gao[1+*], Xueli Sun[2+], Xiongkai Tang[3+], Zhenlang Xie[3], Guolong Tian[3], Zi-Ang Nan[4*], Huayan Yang[4*], and Hui Shen[2*]

[1] School of Chemistry and Chemical Engineering, Yulin University, Yulin 719000, China. Email: gaoyanli8503@126.com.

[2] College of Energy Materials and Chemistry, Inner Mongolia University, Hohhot 010021, China. Email: shen@imu.edu.cn.

[3] State Key Laboratory of Physical Chemistry of Solid Surfaces and College of Chemistry and Chemical Engineering, Xiamen University, Xiamen, 361005, China

[4] School of Biomedical Engineering, Health Science Center, Shenzhen University, Guangdong 518060, China. Email: yanghuayan@szu.edu.cn.

[+] These authors contribute equally to this work.

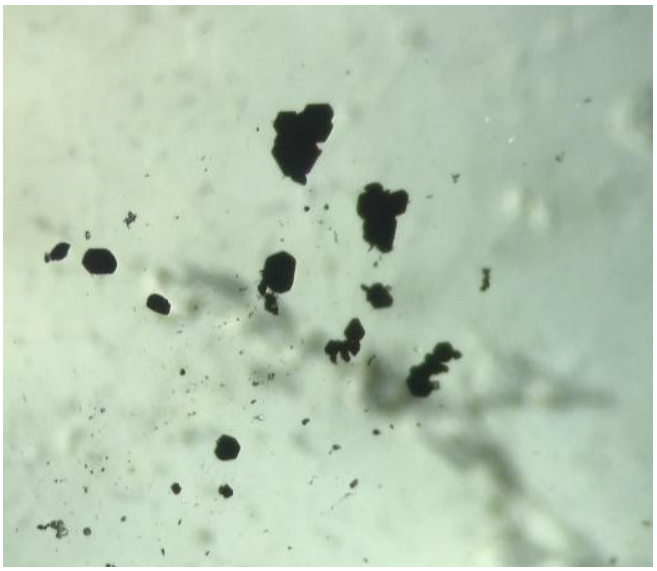

Figure S1. Digital photographs of single crystals of $[Ag_{13-x}Cu_{6+x}(^{t}BuC_6H_4C{\equiv}C)_{14}(PPh_3)_6](SbF_6)_3$ cluster.

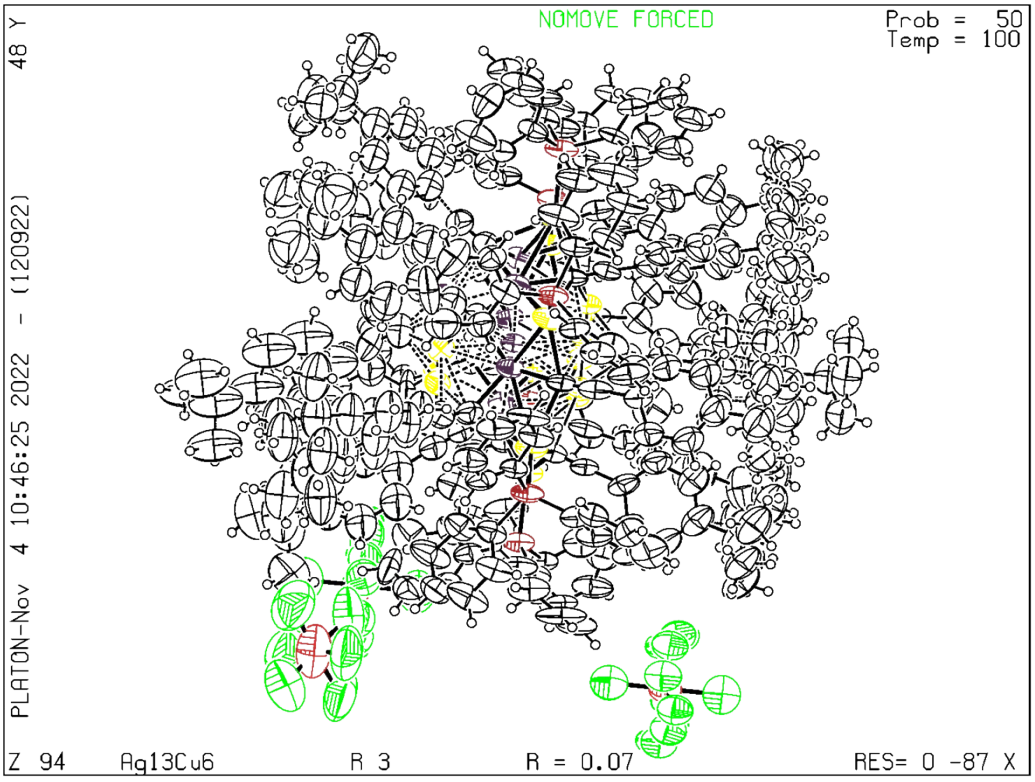

Figure S2. The thermal ellipsoids of the ORTEP diagram of $[Ag_{13-x}Cu_{6+x}(^{t}BuC_6H_4C{\equiv}C)_{14}(PPh_3)_6](SbF_6)_3$ cluster.

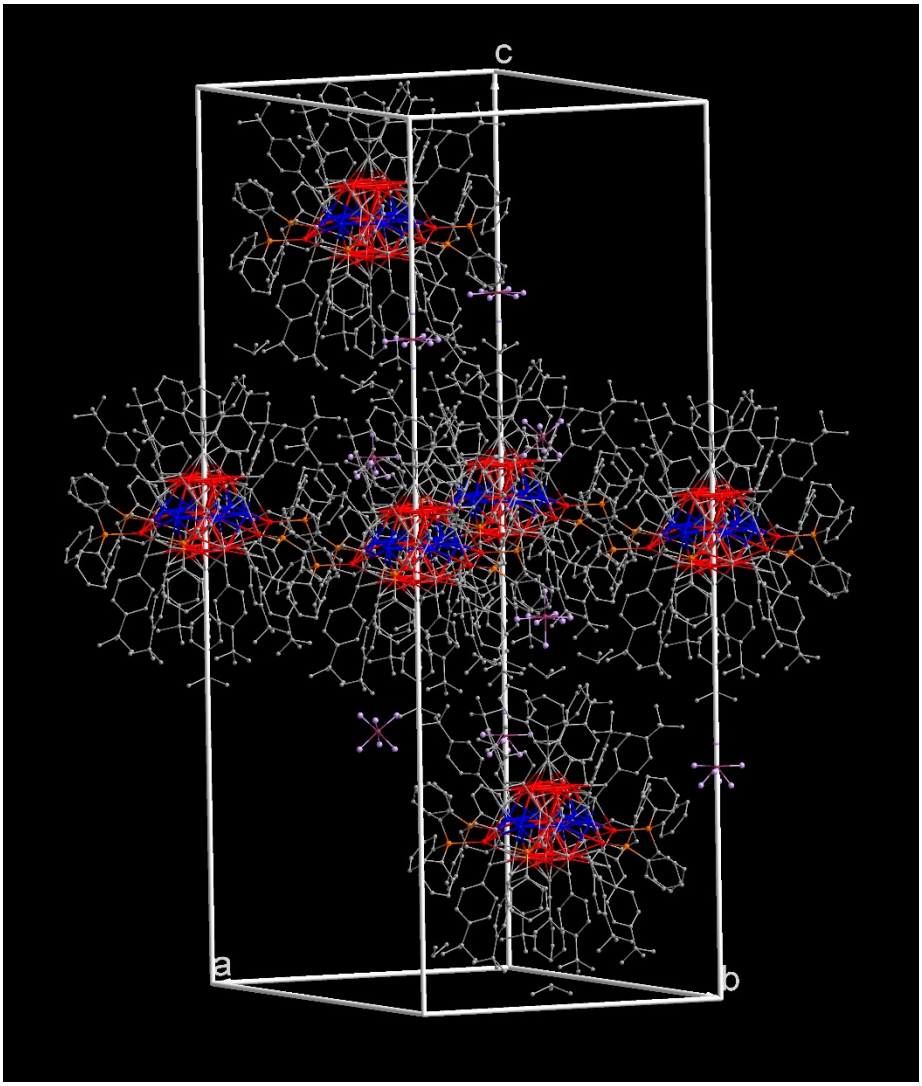

Figure S3. The packing structure of $[Ag_{13-x}Cu_{6+x}(^{t}BuC_6H_4C{\equiv}C)_{14}(PPh_3)_6](SbF_6)_3$ cluster in their single crystals. Color codes for atoms: red spheres, Ag; blue spheres, Cu; orange spheres, P; grey spheres, C; purple spheres, Sb; violet spheres, F. All hydrogen atoms are omitted for clarity.

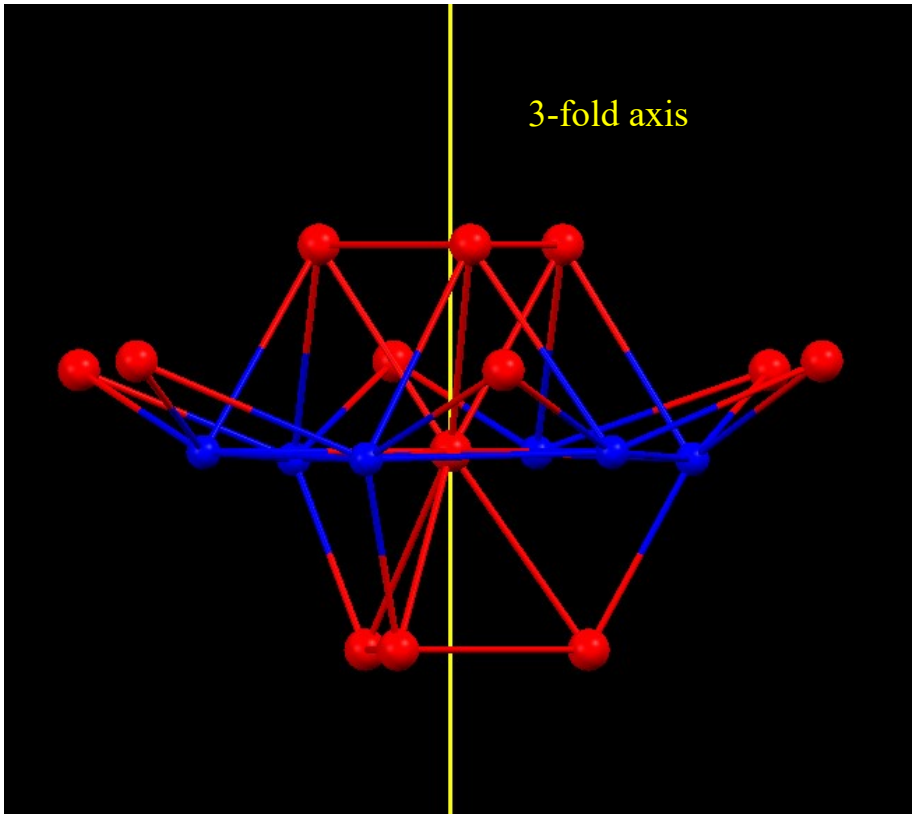

Figure S4. View of 3-fold axis along *a*-axis of $[Ag_{13-x}Cu_{6+x}(^{t}BuC_6H_4C{\equiv}C)_{14}(PPh_3)_6](SbF_6)_3$ cluster. Color codes for atoms: red spheres, Ag; blue spheres, Cu.

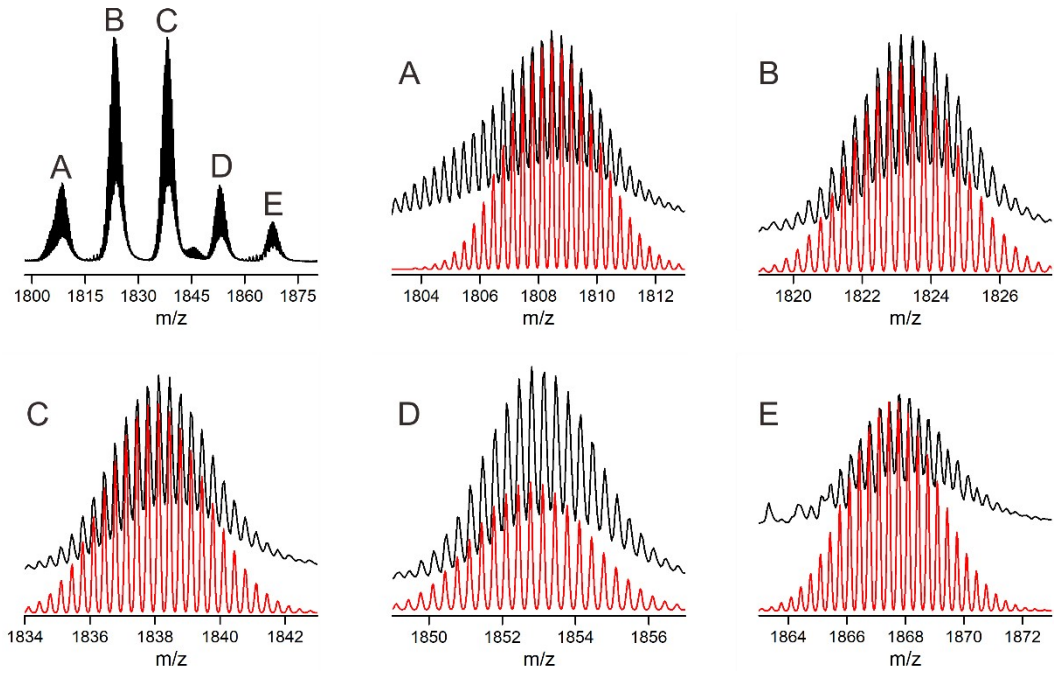

Figure S5. The enlarged ESI-MS spectra of $[Ag_{13-x}Cu_{6+x}(^{t}BuC_6H_4C{\equiv}C)_{14}(PPh_3)_6]^{3+}$ showing the presence of Ag-Cu exchange. From A to E is the experimental and simulated isotopic patterns of the molecular ion peak $[Ag_{13-x}Cu_{6+x}(^{t}BuC_6H_4C{\equiv}C)_{14}(PPh_3)_6]^{3+}$ (x=3, 2, 1, 0, -1), respectively.

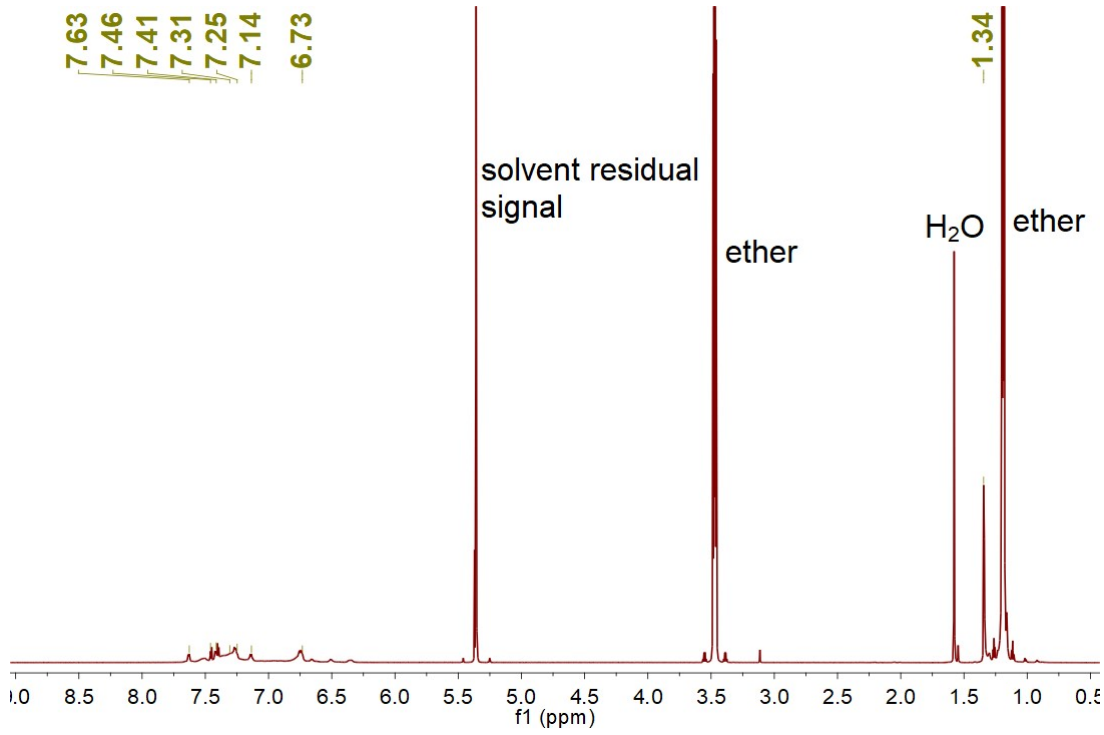

Figure S6. ^{1}H NMR of $[Ag_{13-x}Cu_{6+x}(^{t}BuC_6H_4C{\equiv}C)_{14}(PPh_3)_6](SbF_6)_3$ cluster in CD_2Cl_2.

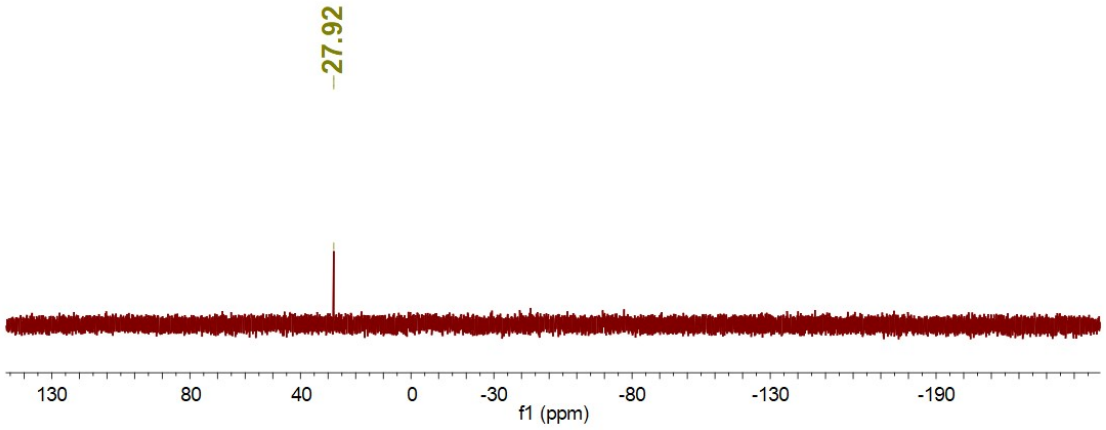

Figure S7. Proton-decoupled ^{31}P NMR of $[Ag_{13-x}Cu_{6+x}(^{t}BuC_6H_4C{\equiv}C)_{14}(PPh_3)_6](SbF_6)_3$ cluster in CD_2Cl_2.

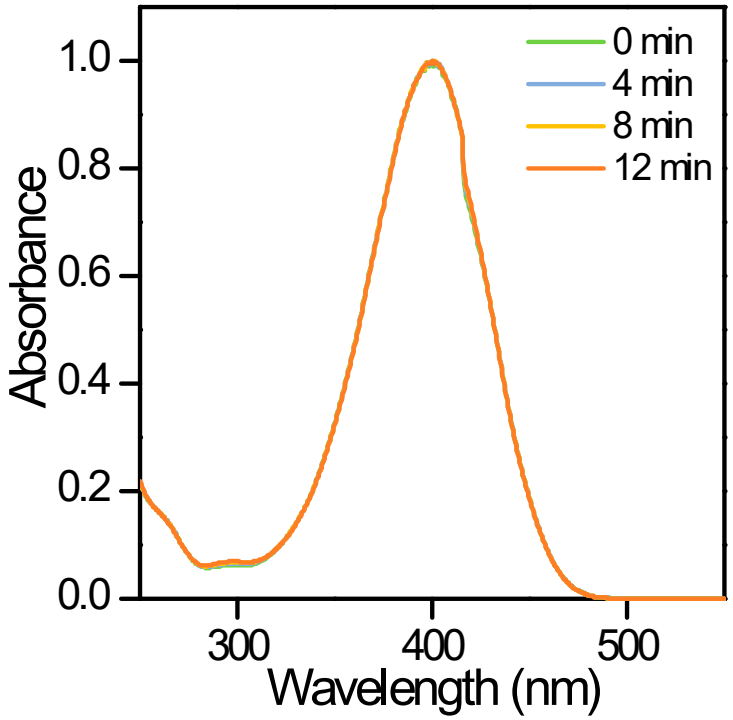

Figure S8. Time-dependent UV-Vis spectra of XC-72 catalyzed reduction of 4-nitrophenol, showing its inertness toward the reaction.

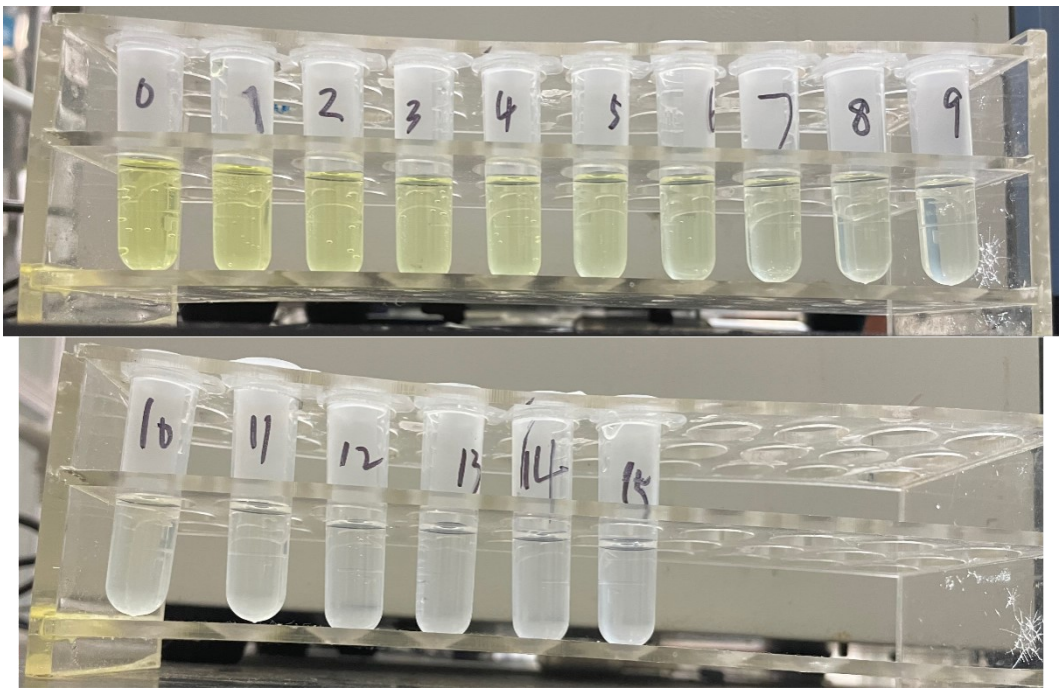

Figure S9. Time-dependent digital photographs of $Ag_{13-x}Cu_{6+x}$/XC-72 catalyzed hydrogenation of 4-nitrophenol.

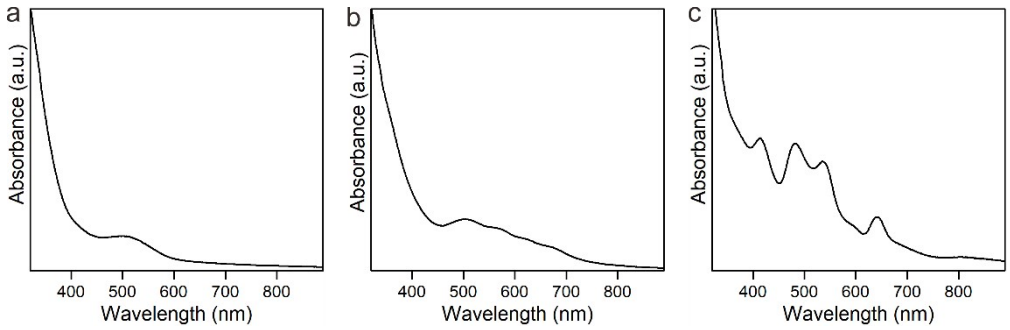

Figure S10. UV-Vis spectra of $[Ag_{25}Cu_4(PhC{\equiv}C)_{12}(PPh_3)_{12}Cl_6H_8](SbF_6)_3$ (a), $[Ag_9Cu_6(^tBuC{\equiv}C)_{12}]SbF_6$ (b) and $Ag_{44}(SC_6H_4CF_3)_{30}$ (c) clusters, respectively.

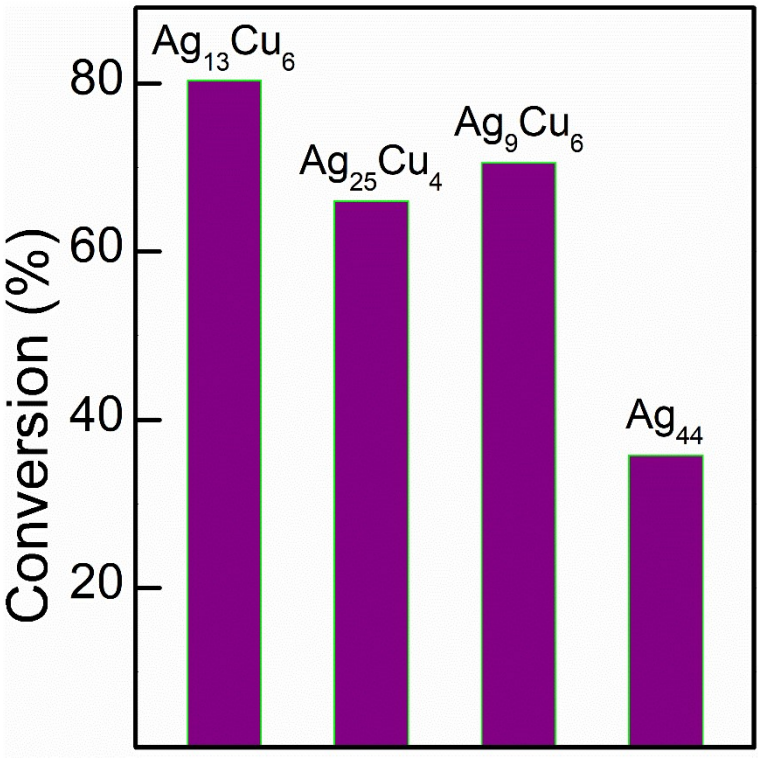

Figure S11. Comparison of catalytic activity of different clusters in hydrogenation of 4-nitrophenol. Note: The conversion was calculated based on the data at 8 min. All the clusters were supported on the XC-72 before catalysis.

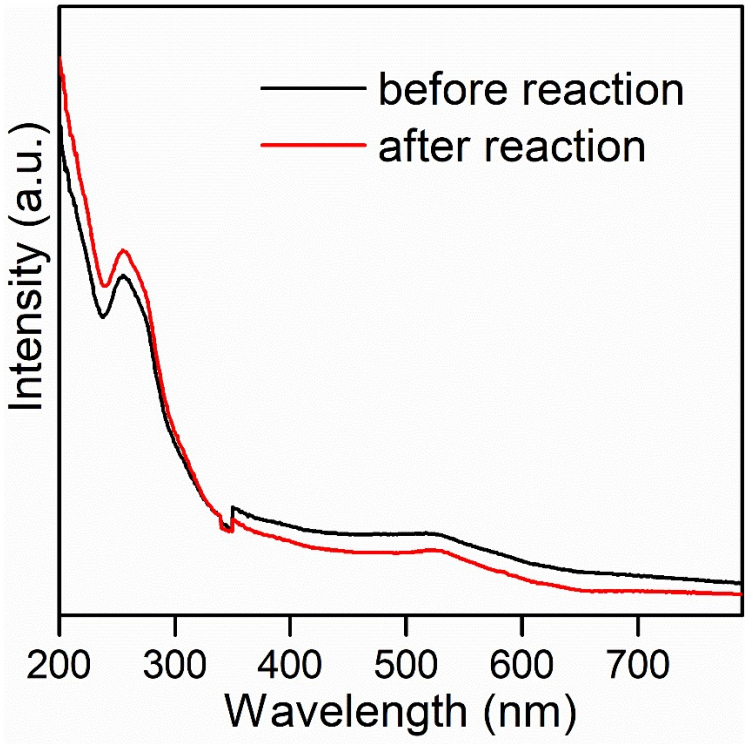

Figure S12. Solid UV-Vis spectra of $Ag_{13-x}Cu_{6+x}/TiO_2$ before and after catalysis in hydrogenation of 4-nitrophenol.

Table S1. Crystallographic data of $[Ag_{13-x}Cu_{6+x}(^tBuC_6H_4C{\equiv}C)_{14}(PPh_3)_6](SbF_6)_3$.

identification code	$[Ag_{13-x}Cu_{6+x}(^tBuC_6H_4C{\equiv}C)_{14}(PPh_3)_6](SbF_6)_3$
formula	$C_{276}H_{272}Ag13\text{-}xCu6\text{+}xP_6F_{18}Sb_3$
formula weight	6265.54
Temperature/K	100.00(10)
crystal system	trigonal
space group	*R*3
a (Å)	20.1767(4)
b (Å)	20.1767(4)
c (Å)	59.918(2)
α (˚)	90
β (˚)	90
γ (˚)	120
V (Å^3)	21124.4(11)
Z	3
D_c / (g·cm^{-3})	1.478
Radiation	Cu Kα (λ= 1.54184 Å)
Theta (˚) range	3.8869 to 64.4100
Index ranges	-23 ≤ h ≤ 22, -23≤ k ≤ 22, -70 ≤ l ≤ 69
Refls. Total	14935
restraints	12084
parameters	1268
R_{int}	0.0466
R_1/wR_2 [I>2σ(I)]	0.0774 0.2105
R_1/wR_2 (all data)	0.0895 0.2360
completeness	0.9996
GooF	1.034

Table S2 Selected bond lengths (Å) for cluster $Ag_{13-x}Cu_{6+x}$.

Parameter	value	Parameter	value
Ag01-Ag05	2.856(2)	Ag05-C01N	2.441(14)
Ag01-Ag0B	2.845(4)	Cu08-C013	2.178(19)
Ag01-Ag00	2.764(9)	Cu08-C01D	1.98(2)
Ag02-Cu08	2.654(2)	Cu08-C01N	1.954(18)
Ag02-Cu09	2.846(3)	Cu09-Cu08	2.820(3)
Ag02-P0C	2.385(4)	Cu08-Cu09	2.837(3)
Ag02-C00Z	2.44(3)	Cu09-Ag00	2.500(10)
Ag02-C01D	2.59(2)	Cu09-C00Z	2.00(3)
Ag02 C01N	2.432(14)	Cu09-C013	1.98(2)
Ag03-Ag05	3.293(2)	Cu09-C01D	2.13(2)
Ag03-Cu08	2.818(2)	Ag00-Ag00	2.737(14)
Ag03-Cu09	2.678(2)	Ag00-C013	2.33(2)
Ag03-P00D	2.389(4)	Ag00-C01D	2.34(2)
Ag03-C00Z	2.40(3)	Ag00-C01R	2.53(2)
Ag03-C013	2.548(16)	Ag05-Cu08	2.919(3)
Ag03-C01N	2.500(13)	Ag05-Cu09	2.895(3)
Ag05-Ag05	2.809(3)	Ag05-C00Y	2.28(2)
Ag05-Ag05	2.809(3)	Ag05-C00Z	2.41(2)

Table S3 Selected angles (°) for cluster $Ag_{13-x}Cu_{6+x}$.

Parameter	value	Parameter	value
Ag05-Ag01-Ag05	58.90(6)	Ag01-Ag05-Ag03	98.82(6)
Cu09-Ag01-Ag05	61.62(7)	Ag01-Ag05-Cu08	59.35(6)
Cu09-Ag01-Ag05	120.47(8)	Ag01-Ag05-Cu09	58.16(6)
Cu09-Ag01-Ag05	92.45(7)	Ag05-Ag05-Ag01	60.55(3)
Ag00-Ag00-Ag01	60.32(15)	Ag05-Ag05-Ag03	140.76(7)
Cu09-Ag01-Cu09	119.910(8)	Ag05-Ag05-Ag03	141.73(7)
Ag00-Ag01-Ag05	113.32(19)	Ag05-Ag05-Ag05	60.0
Ag00-Ag01-Ag05	163.3(2)	Ag05-Ag05-Cu08	88.79(7)
Ag00-Ag01-Ag05	132.2(2)	Ag05-Ag05-Cu08	119.87(5)
Ag00-Ag01-Cu09	103.9(2)	Ag05-Ag05-Cu09	118.67(5)
Ag00-Ag01-Cu09	106.3(2)	Ag05-Ag05-Cu09	91.36(7)
Ag00-Ag01-Cu09	53.43(19)	Cu08-Ag05-Ag03	53.54(6)
Ag00-Ag01-Ag00	59.4(3)	Ag01-Cu08-Ag05	59.24(6)
Cu08-Ag02-Cu09	61.58(7)	Ag02-Cu08-Ag01	115.71(8)
P0C-Ag02-Cu08	145.94(14)	Ag02-Cu08-Ag03	115.09(10)
P0C-Ag02-Cu09	133.03(13)	Ag02-Cu08-Ag05	98.35(9)
P00D-Ag03-Ag05	153.03(15)	Ag02-Cu08-Cu09	158.38(12)
P00D-Ag03-Cu08	132.43(13)	Ag02-Cu08-Cu09	62.56(7)
P00D-Ag03-Cu09	148.61(14)	Ag03-Cu08-Ag01	110.97(8)
Cu09-Ag05-Ag03	50.78(6)	Ag03-Cu08-Ag05	70.04(7)
Cu09-Ag05-Cu08	58.41(7)	Ag03-Cu08-Cu09	56.53(6)
Ag01-Cu09-Ag02	111.71(8)	Ag03-Cu08-Cu09	160.30(12)
Ag01-Cu09-Ag05	60.22(6)	Cu09-Cu08-Ag01	58.98(6)
Ag01-Cu09-Cu08	61.01(6)	Cu09-Cu08-Ag05	90.64(9)
Ag02-Cu09-Ag05	94.28(9)	Ag02-Cu09-Ag05	94.28(9)
Ag03-Cu09-Ag01	117.43(8)	Ag00-Cu09-Ag03	125.3(3)
Cu08-Cu09-Cu08	122.20(11)	Ag00-Cu09-Ag05	120.8(2)
Ag00-Cu09-Ag01	62.6(2)	Ag00-Cu09-Cu08	79.0(3)
Ag00-Cu09-Ag02	120.2(3)	Ag00-Cu09-Cu08	76.5(2)
Ag00-Ag00-Ag00	60.001(4)		